Image quality and radiation dose of dual-source CT cardiac angiography using prospective ECG-triggering technique in pediatric patients with congenital heart disease

Department of Radiology, Xijing Hospital, Fourth Military Medical University, 169 West Changle Road, Xi'an 710032, China

Background:

-Sequential scanning technique with prospective ECG triggering could help to reduce the radiation exposure in cardiovascular CT.

-Prospective ECG gating only allows the ionized X-ray radiation to apply at a certain predefined period of the cardiac cycle rather than during the entire cycle as compared to retrospective ECG-gating technique.

-Retrospective ECG gating scans the patient continuously at all phases of the cardiac cycle, although only certain portions of the scan are used to reconstruct the image, causing higher dose of radiation to patient.

Purpose of study:

-To evaluate the image quality and diagnostic accuracy of DSCT cardiac angiography using low-voltage prospective ECG-triggering technique in pediatric patients with congenital heart disease in comparison with non-ECG-gated technique.

-To determine whether dual source CT (DSCT) cardiovascular angiography using prospective ECG-triggering can be performed in pediatric patients with congenital heart disease.

Method:

-60 pediatric patients younger than 5 years old were included in this study.

-Referred for DSCT angiography for evaluation of suspected congenital cardiovascular anomalies for clinical reasons.

-Final diagnosis of congenital heart disease was based on the surgical and/or conventional cardiac angiography findings.

-All patients were randomly assigned to two groups for DSCT angiography (with 30 patients in each group).

-Patients in group A were scanned using prospective ECG-triggering.

-Patients in group B were examined by non-ECG-gated spiral CT scans.

Parameter	Group A	Group B
Number of children	30	30
Sex (male/female)	17/13	14/16
Mean age (Y)	2.6 ± 2.4	2.2 ± 1.8
Mean weight (Kg)	7.3 ± 7.1	7.1 ± 6.7
Tube voltage (kV)	80	80
Tube current time (mAs)	250	250
Collimation (mm)	0.6	0.6
Rotation time (sec)	0.33	0.50
Pitch	NA	1.0
Slice thickness (mm)	1.0	1.0
Reconstruction interval (mm)	0.8	0.8

CT cardiac angiography protocol in HUSM (<5years old)

Somatom Definition AS Plus

-Tube voltage: 80kV

-Tube current time: 250mAs

-Collimation: 0.75mm

-Rotation time: 0.3s

-Slice thickness: 1.5mm

-Pitch: 1.4

-Prospectively ECG gated

Dual Source CT Protocol:

-All CT examinations were performed on a DSCT scanner (SOMATOM Definition, Siemens Medical Solutions, Forchheim, Germany).

-All patients were put under sedation by oral administration of chloral hydrate (50 ~ 75 mg/kg) according to the patient's body weight and clinical condition.

-Abdominal bandage was used to reduce the respiratory artifacts during CT scan.

-Scanned in a cranio-caudal direction from the lung apex to the liver dome to cover the entire lung parenchyma.

 -2 ml/kg of Iopamiro 370 mg I/mL, was injected through a peripheral venous line by using a power injection.

-Followed by 20 ml of saline flush.

-Flow rate of 0.5 ~ 2.0 ml/s.

-A round region of interest (ROI) was placed in the left ventricle (ROI was set at 100 HU).

-Prospectively ECG-triggered, starting at 40 % of the R-R interval.

-Multiplanar reformation (MPR), maximum intensity projection (MIP) and volume rendering technique (VRT) were used to visualize cardiovascular abnormalities.

-The CT volume dose index (CTDIvol) and dose-length product (DLP) values were recorded from the CT console displays for each scan. The effective dose was derived from the product of DLP and a conversion coefficient of 0.021 mSv/[mGy · cm] for the pediatric chest.

Results:

-Diagnoses of cardiac abnormalities were proved by the surgical and/or conventional cardiac angiography.

-A total of 106 separate cardiovascular abnormalities were confirmed by surgical and/or CCA findings in Group A, and 102 abnormalities in Group B.

-The total diagnostic accuracy of prospective ECG- triggering scan and non-ECG-gated scan was 97.2 % (103/106) and 90.2 % (92/102), respectively, which was significantly higher in group A than in group B (P = 0.011).

Table 3 Cardiovascular deformity findings with prospective ECG-triggering DSCT angiography (Group A) and non-ECG-gated DSCT (Group B) with reference to surgical and/or CCA findings

Abnormalities	Group A/surgery and/or CCA	Group B/surgery and/or CCA
Atrial septal defect	18/19	18/21
Ventricular septal defect	18/18	18/19
Patent ductus arteriosus	16/16	14/14
Aortic pulmonary septal defect	1/1	0/1
Anomalous pulmonary venous return	5/5	3/3
Aortic coarctation	6/6	8/8
Interrupted aortic arch	2/2	2/3
Coronary artery anomaly	2/2	0/1
Right aortic arch	0/0	2/2
Pulmonary valve stenosis	2/4	1/2
Pulmonary artery stenosis	11/11	9/9
Pulmonary artery atresia	4/4	2/3
Dilated pulmonary artery	11/11	9/9
Anomalous origin of pulmonary artey	3/3	2/2
Transposition of the great arteries	2/2	3/3
Double outlet right ventricle	2/2	1/2
Total	103/106	92/102

Evaluation of image quality:

-Two cardiovascular radiologists (with 7 and 10 years experience, respectively) subjectively interpreted image quality.

-A 5-point scale was used to grade the image quality (5 = excellent; 4 = good; 3 = fair; 2 = poor; 1 = not applicable)

-The image quality with prospective ECG-triggering acquisition was found to be significantly better than with non-ECG gated spiral acquisition.

-With good agreement ($κ = 0.73$) for overall image quality scoring between the two reviewers.

Radiation dose:

Table 5 Radiation dose parameters of prospective ECG-triggering DSCT (Group A) and non-ECG-gated DSCT (Group B)

	Group A	Group B	P value
$CTDI_{vol}$ (mGy)	1.58 ± 0.65	1.39 ± 0.71	0.519
DLP (mGy·cm)	19.71 ± 10.56	22.29 ± 13.00	0.560
Effective radiation dose (mSv)	0.41 ± 0.22	0.47 ± 0.27	0.560

$CTDI_{vol}$, volume CT dose index; DLP, dose-length product

Discussion:

-Any diagnostic test with ionizing radiation should be performed in accordance with the ALARA (As Low As Reasonably Achievable) principle, especially in children.

-With the conventional non-ECG-gated DSCT scan, infants and children who can't hold their breath during CT scans, motion artifact has always been an issue and can severely impair the image quality and also lower the diagnostic accuracy.

-In order to reduce radiation dose while maintain the image quality, many dose-saving techniques have been developed, e.g., ECG-controlled dose modulation, tube voltage reduction and prospective gating sequential scanning mode.

-Among these strategies, prospective ECG-triggering DSCT is considered one of the most useful methods to reduce radiation dose.

-X-ray exposure only occurs during the selected cardiac phase rather than throughout the entire cardiac cycle.

Conclusion:

-Results from this study showed that with low tube voltage (80 kV) there was slightly lower effective radiation dose of the prospective ECG-triggering DSCT scan group (0.41 ± 0.22 mSv) compared non-ECG-gated DSCT scan group (0.47 ± 0.27 mSv) ($P = 0.560$).

-However, the image quality score of prospective ECG triggering DSCT scan group (4.4 ± 0.1) is significantly better than that of non-ECG-gated DSCT scan group (3.8 ± 0.3) ($P = 0.007$).

-In accordance with the image quality, the diagnostic accuracy of prospective ECG triggering DSCT scan group (97.2 % (103/106)) is also significantly better than that of non-ECG-gated DSCT scan group (90.2 % (92/102)) ($P = 0.011$)

Cardiothoracic Imaging

Diastolic and systolic right ventricular diameters for predicting pulmonary hypertension in children with congenital heart disease

Bow Wang [a], Li-Ting Huang [a], Min-Ling Hsieh [b], Chien-Kuo Wang [a], Jieh-neng Wang [b], Chung-Dann Kan [c], Jing-Ming Wu [b], Yi-Shan Tsai [a,*]

Supervisor : Dr Khairil Amir Sayuti

Presenter   : Dr. Mohd Nur Naim Bin Che Wil

Date   : 4.1.2021

Source   : Clinical imaging volume 70 (Elsevier INC)

Introduction

- Echocardiography is traditionally the first-line imaging modality used for patients with congenital heart disease (CHD).

- Pulmonary hypertension (PH) in adult is defined as an increase in mean pulmonary arterial pressure (PAP) > 20 mm Hg to 25 mm Hg at rest

- Right ventricular (RV) function determines both the degree of symptoms and survival among patients with PH, and RV failure remains the common fatal pathway and consequence of PH

- Although defining PH is currently based on invasive cardiac catheterization, transthoracic echocardiogram is the initial diagnostic tool used to confirm suspicions of elevated pulmonary pressure when PASP is above 40 mm Hg

Introduction

- Multidetector CT (MDCT) has been used increasingly for imaging patients with CHD, because it provides high-quality three-dimensional images enabling evaluation of complex heart structures

- In pediatric patients, indications for CT are CHD with complex and heterogeneous nature needing detailed assessment
  - associated with abnormal coronary arteries, including transposition of the great arteries [TGA], tetralogy of Fallot [TOF], truncus arteriosus and double-inlet left ventricle

- Previous studies have reported that several parameters obtained with cardiac magnetic resonance imaging and CT,), can be used to predict PH in adults
  - including the ratio of the main pulmonary artery (MPA) and the ascending aorta diameters (AA), the right ventricular maximal diameter, the ratio of right and left ventricular diameters, the ratio of right and left ventricular volumes, and the septal eccentricity index (SEI)

Introduction

- To date, only few studies have presented useful parameters for predicting PH in children
  - Eg: CT measured MPA/AA of 1.3 was identified to be indicative of PAH in children by using non-gating 64-slice MDCT
- Prospective ECG gated cardiac CTA (step-and-shoot mode) is widely used
  - lower radiation dose compared ECG-gated technique
- Previous studies shown for neonates and young children (morphological and proximal coronary artery detail)
  - prospective ECG triggered technique may be used to reduce the radiation dose and motion artifacts

Purpose

- Functional parameters acquired using prospective ECG-gated cardiac CT to predict PH in children with CHD have not yet been reported

- Therefore, this study aimed to investigate the potential of parameters from prospective ECG-gated cardiac CTA to predict PH in children with CHD

Study design and population

- Single-center (National Cheng Kung University Hospital, Taiwan), retrospective.

- approved by the institutional review board (IRB) of the hospital

- requirement for signed informed consent was waived due to the retrospective analysis and deidentification of patients.

Inclusion:
- CHD patients received prospective ECG-triggered cardiac CT angiography
- Age < 20y/o

N=233

Exclusion:
- CHD patients with right chambers involvement
- No cardiac echo within 3 months (71)
- Condition change within 3 months (8)

N=154

Exclusion:
- Right ventricular outlet obstruction (RVOTO) (45)
- Pulmonary arterial stenosis (PS) (38)

N=81

Exclusion:
- PASP data unavailable (17) (Assisted by pediatric cardiologist)

N=64

Exclusion:
- No CT raw data (9)
- Suboptimal image study (11)

Final study population (N=44)
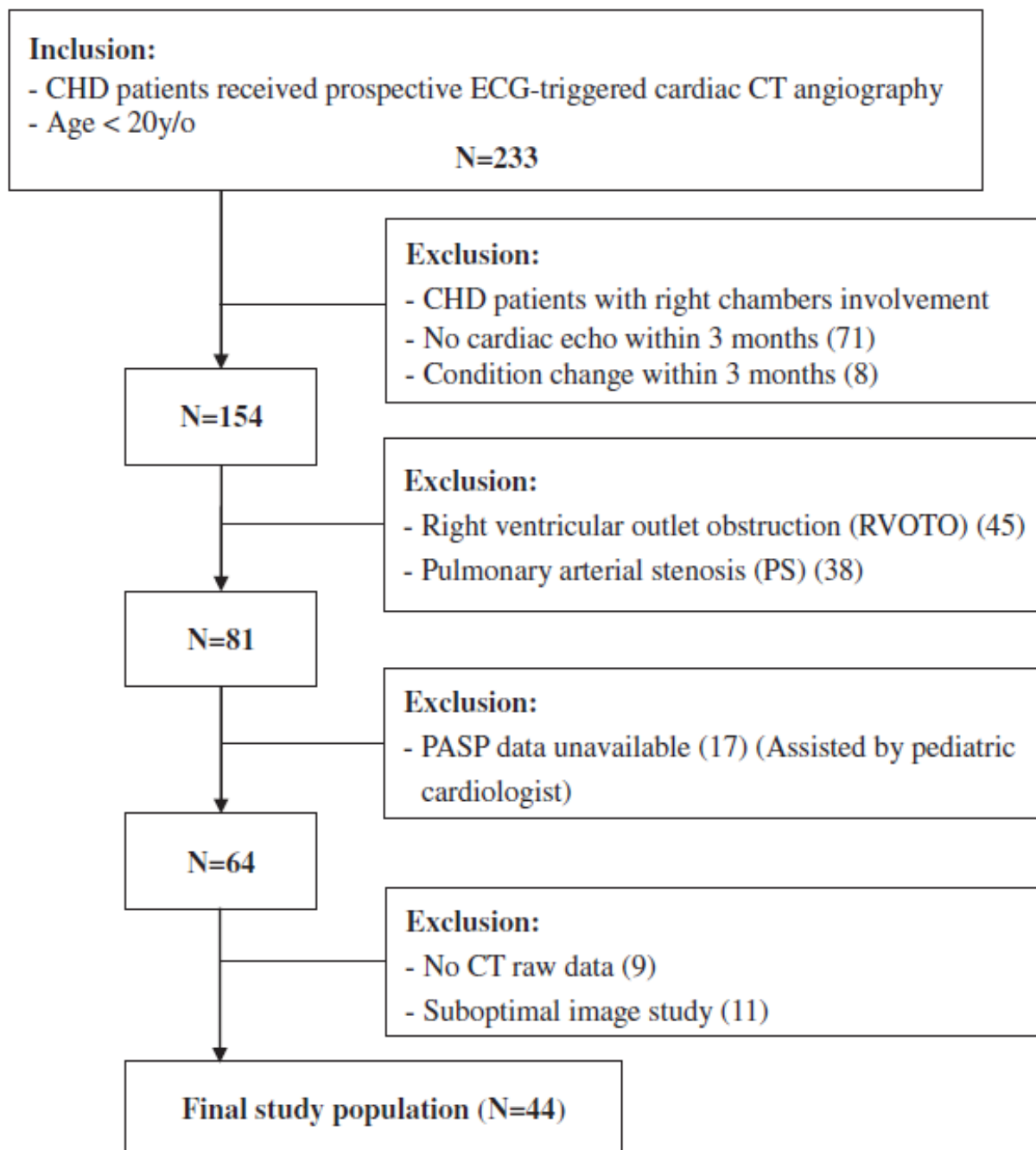
Fig. 1. Flow chart of the study population.

Prospective ECG-gated cardiac CT protocol

- Cardiac CT was performed with a dual-source CT system (Somatom Definition Flash; Siemens Healthcare, Forchheim, Germany) using the prospective ECG-gated scan mode (step-and-shoot scan mode).

- detector collimation, 2 × 64 × 0.6 mm; slice acquisition, 2 × 128 × 0.6 mm using a z-flying focal spot; gantry rotation time, 280 ms; quality reference mAs, 150 per rotation; and tube voltage, 80 kV

- minimum cycle time of 1.36 s for one acquisition and a subsequent table feed were required, and the temporal resolution was 75 ms.

- patients who were unable to obey commands were sedated through oral or anal administration of chloral hydrate

- scanned in a craniocaudal direction from the shoulder to the liver dome, to ensure inclusion of the subclavian artery and entire lung parenchyma.

- nonionic contrast medium iopromide (Ultravist® 30, 370 mg/ml), 2–3 ml/kg contrast medium (CM), followed by a normal saline flush

- flow rate of 0.3–2.0 ml/s according to the size of intravenous access
- round region of interest (ROI) was defined in the descending aorta selected for optimum vascular opacification
- triggered threshold ROI: 100 HU, image scan began after a delay of 7–9 s
- data acquisition window center was set at 70% and 30% of the R-R interval for diastole and systole, respectively
- interval between two consecutive scans was 5 s limited by the change in scan parameters and the table movement

CT image analysis

- One-millimeter thin-slice CTA images were analyzed using semiautomated postprocessing three-dimensional viewer software (Aquarius iNtuition Edition Ver: 4.4.7; TeraRecon, San Mateo, CA)

- selected parameters were analyzed by 2 independent readers:
  - B. W. and Y.S.T., with 3 and 14 years of experience in cardiothoracic imaging

- images were initially analyzed by an experienced cardiac radiologist, including disease classification

- Measurements of parameters for the images were performed by a pediatric radiologist

- To determine the intra-observer variability, the same pediatric radiologist analyzed the images for all patients 1 month later.

- first and second analyses were averaged to minimize intra-observer variability

- an experienced cardiac radiologist, who was blinded to the initial analysis, re-evaluated the images of 50% of the patients, who were chosen at random, to determine interobserver variability

Modified ventricular diameter and cross-sectional area

- user-selected short-axis two-chamber view was reformed to be perpendicular to the long axis of the left ventricle (LV) (30% and 70% of the R-R interval)

- plane was moved until the papillary muscle was no longer visible, and a user selected apical four-chamber view was then reformed to visualize according to an ideal right-ventricle focused view defined in a guideline on right-heart evaluation maximal ventricular diameter and cross-sectional area (CSA), according to an ideal right-ventricle focused view defined in a guideline on right-heart evaluation

- modified diameter and CSA were calculated as the RVD and LVD divided by the body surface area (BSA) and the RVCSA and LVCSA divided by the BSA, respectively; measurements were obtained in both systole and diastole

A

B

C

D

18.0 mm   23.1 mm
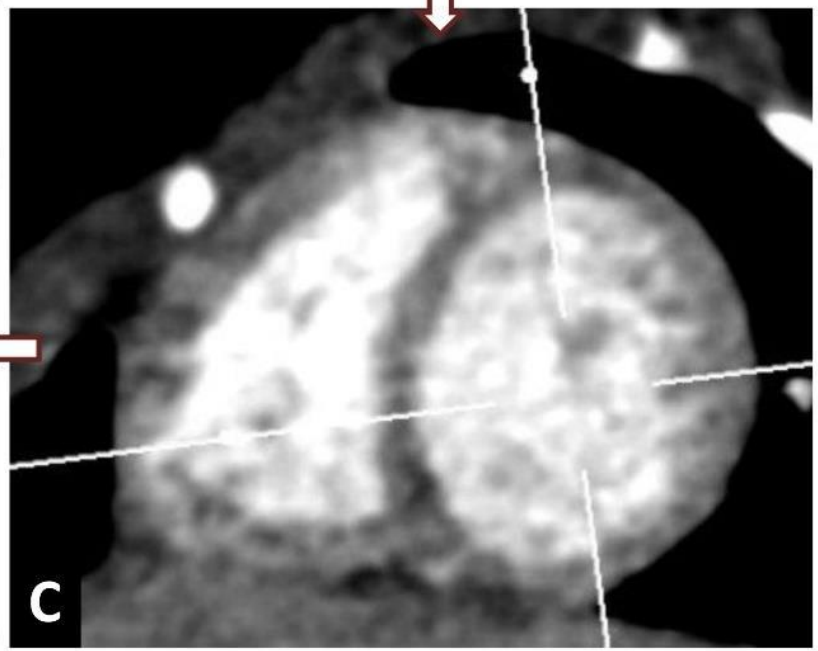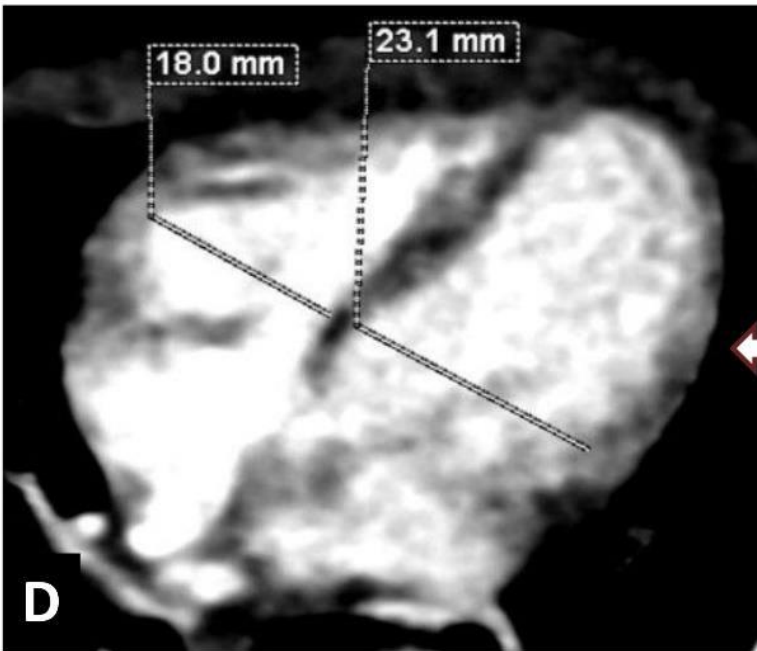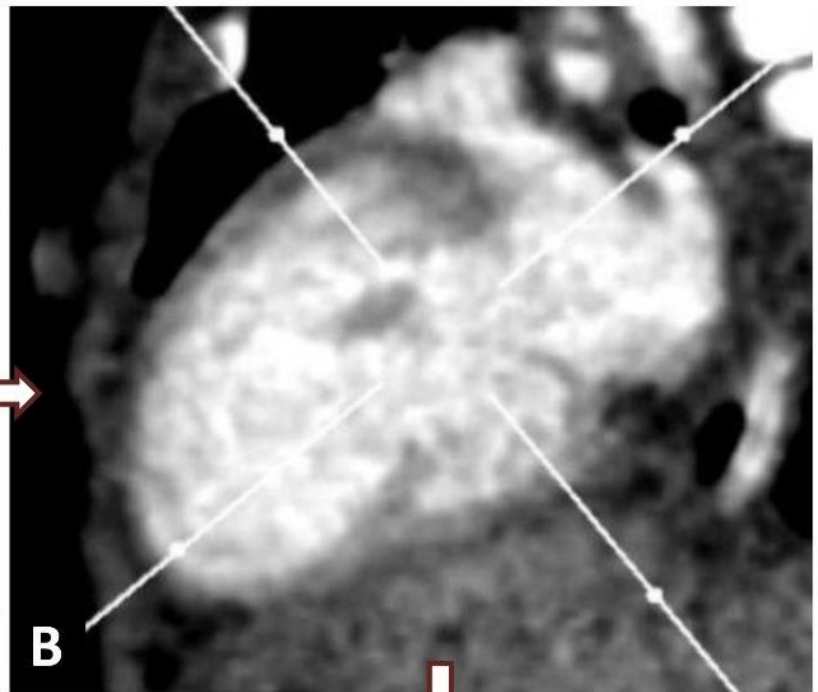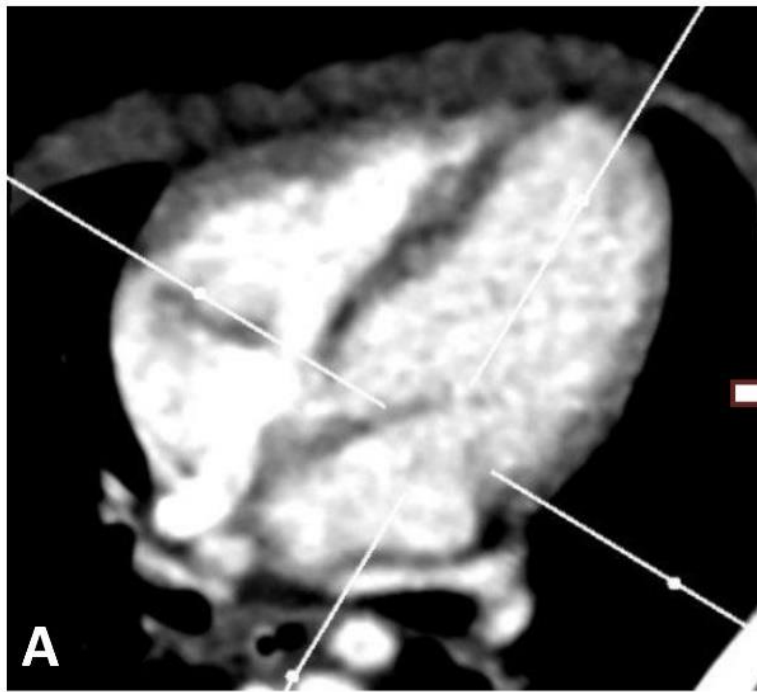
Ventricular diameter and CSA ratios

- The RVD/LVD and RVCSA/LVCSA ratios were calculated in both systole and diastole

Septal eccentricity index (SEI)

- defined as SI/AP dimension (D2/D1) in which higher SEI reflects higher PA pressure, with reported thresholds for PH (>1.3)

- SEI was calculated as the ratio of the distance between the septal–lateral wall and the anterior–posterior wall measured in the short-axis view

- Diameter measurements were obtained from the short-axis two-chamber view, which was adjusted at the mitral chordal insertion level

A

B

C

D

24.4 mm

30.2 mm
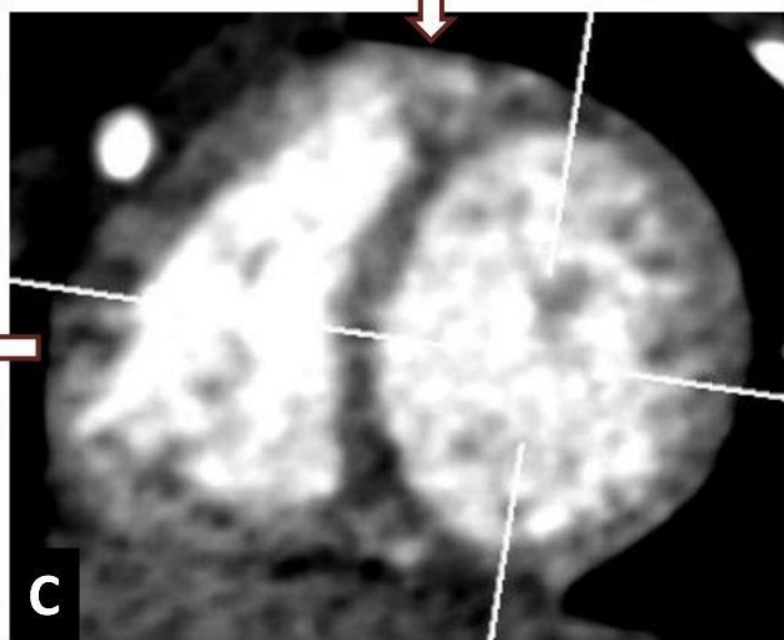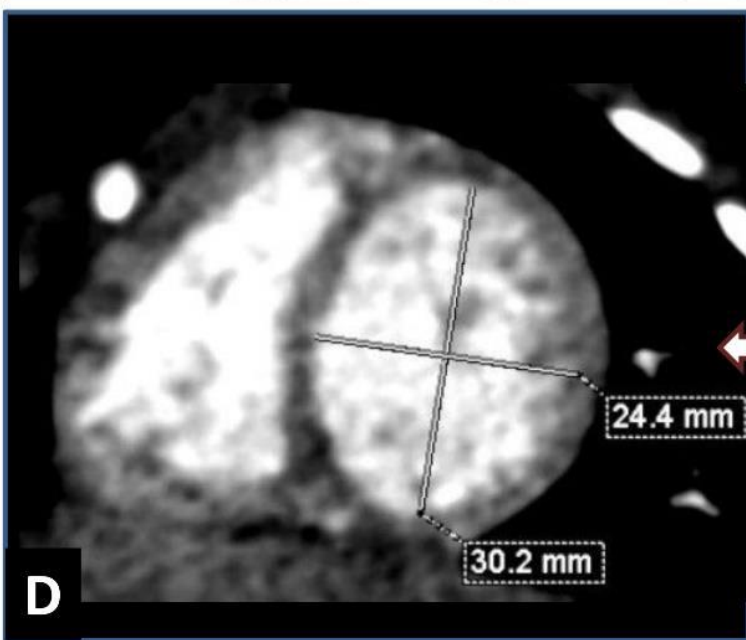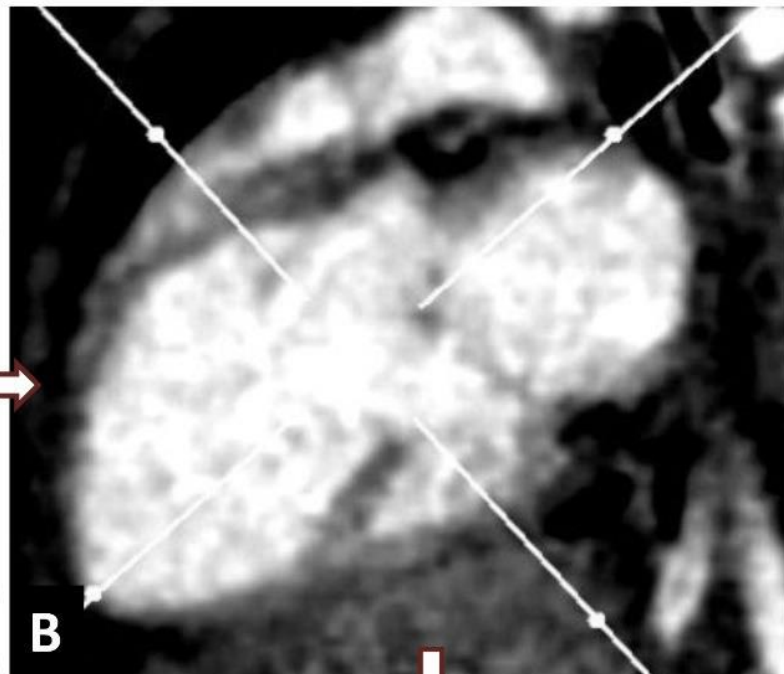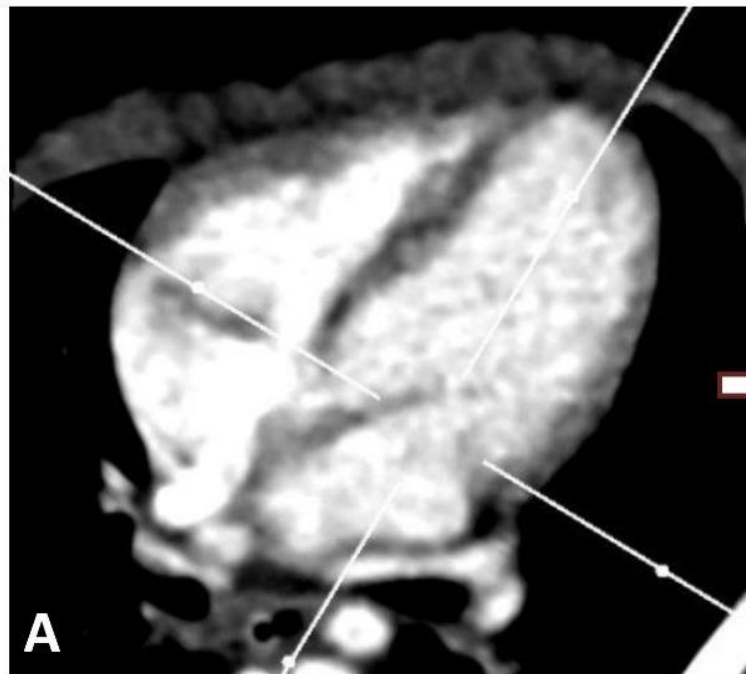
Interobserver agreement and intrarater reliability

- Good to excellent agreement between the results of the two observers was attained regarding functional parameters in the cardiac CT scans of 44 patients (Cohen's Kappa 0.625–0.821)

- Consistency of one observer's measurements of functional parameters was good (Pearson correlation coefficient: 0.772–0.980).

Radiation dose

- effective dose in millisieverts was estimated by multiplying the dose-length product (DLP) by 2.3
- effective radiation dose delivered during a chest CTA was calculated using International Commission on Radiological Protection publication 103 to determine the CT conversion factor
- Conversion factors: 0.0823 for newborns, 0.0525 for 1-year old infants, 0.0344 for children aged 1–5 years, 0.0248 for children aged 5–10 years, and 0.0147 for children older than 10 years, based on a scan tube voltage of 80

Statistical analysis

- Continuous variables are presented as mean and standard deviations (SDs) for normal distribution and tested by t-test or median and interquartile range (IQR) for non-normal distribution and tested by Kruskal- Wallis test

- Categorical variables are presented as counts and percentages and tested by Chi-square test or Fisher's Exact test

- Associations between measured parameters and PH were evaluated by logistic regression and baseline characteristics that were significantly different between the PH group and non-PH group were selected into multivariate logistic regression for adjustment

- receiver operating characteristic (ROC) curve was used to find the best cut-off point for parameters measured by Youden's index

Statistical analysis -cont

- Interrater reliability (IRR) was assessed using Kappa statistics
  - IRR was poor, fair, good, and excellent for Cohen's Kappa values from 0.0 to 0.2 indicating slight agreement
  - 0.21 to 0.40 indicating fair agreement
  - 0.41 to 0.60 indicating moderate agreement
  - 0.61 to 0.80 indicating substantial agreement
  - 0.81 to 1.0 indicating almost perfect or perfect agreement
- intrarater reliability was evaluated on the basis of test–retest reliability, and a Pearson correlation coefficient of >0.7 indicated good consistency
- statistical analyses were two-tailed and were performed using SAS version 9.4
- p value of <0.005 was established as statistical significance

Table 1

Characteristics of the study population.

Variable	Non-PH group N = 22	PH group N = 22	p-Value
Age, months	36 (8, 84)	1 (0.13, 5)	<0.0001[a,*]
Sex			
Female	11 (50%)	10 (45.45%)	0.76[b]
Male	11 (50%)	12 (54.55%)	
Diagnosis			
ASD	7 (31.82%)	13 (59.09%)	0.07[b]
VSD	10 (45.45%)	16 (72.73%)	0.07[b]
CoA	3 (13.64%)	4 (18.18%)	1.00[c]
PDA	2 (9.09%)	10 (45.45%)	0.01[b,*]
TAPVR/PAPVR	2 (9.09%)	3 (13.64%)	1.00[c]
PASP	25.45 ± 8.44	58.41 ± 10.39	<0.0001[d,*]
D-RVD-BSA	5.02 ± 1.86	9.22 ± 2.87	<0.0001[d,*]
D-LVD-BSA	5.57 ± 2.38	8.77 ± 2.38	<0.0001[d,*]
D-RVCSA-BSA	18.79 ± 6.52	23.45 ± 7.87	0.04[d,*]
D-LVCSA-BSA	21.07 (18.84, 25.15)	22.39 (19.64, 31.34)	0.36[a]
D-RVD/LVD	0.88 (0.74, 1.08)	1.01 (0.85, 1.13)	0.26[a]
D-RVCSA/LVCSA	0.71 (0.55, 1.21)	0.83 (0.66, 0.98)	0.28[a]
D-SEI	0.81 ± 0.11	0.75 ± 0.16	0.18[d]
D-MPA/Ao	1.13 (1.08, 1.24)	1.56 (1.26, 1.72)	0.0001[a,*]
S-RVD-BSA	4.62 ± 1.58	8.21 ± 2.39	<0.0001[d,*]
S-LVD-BSA	4.55 ± 2.14	6.87 ± 1.81	0.0004[d,*]
S-RVCSA-BSA	8.98 (5.68, 12.25)	3.99 (3.44, 5.08)	0.001[a,*]
S-LVCSA-BSA	8.45 (6.06, 13.85)	4.20 (2.48, 5.26)	0.0002[a,*]
S-RVD/LVD	0.96 (0.89, 1.19)	1.07 (0.99, 1.32)	0.05[a]
S-RVCSA/LVCSA	0.86 (0.74, 1.19)	0.89 (0.81, 1.29)	0.31[a]
S-SEI	0.90 ± 0.09	0.79 ± 0.19	0.02[d,*]
S-MPA/Ao	1.19 (1.10, 1.26)	1.66 (1.46, 1.84)	<0.0001[a,*]

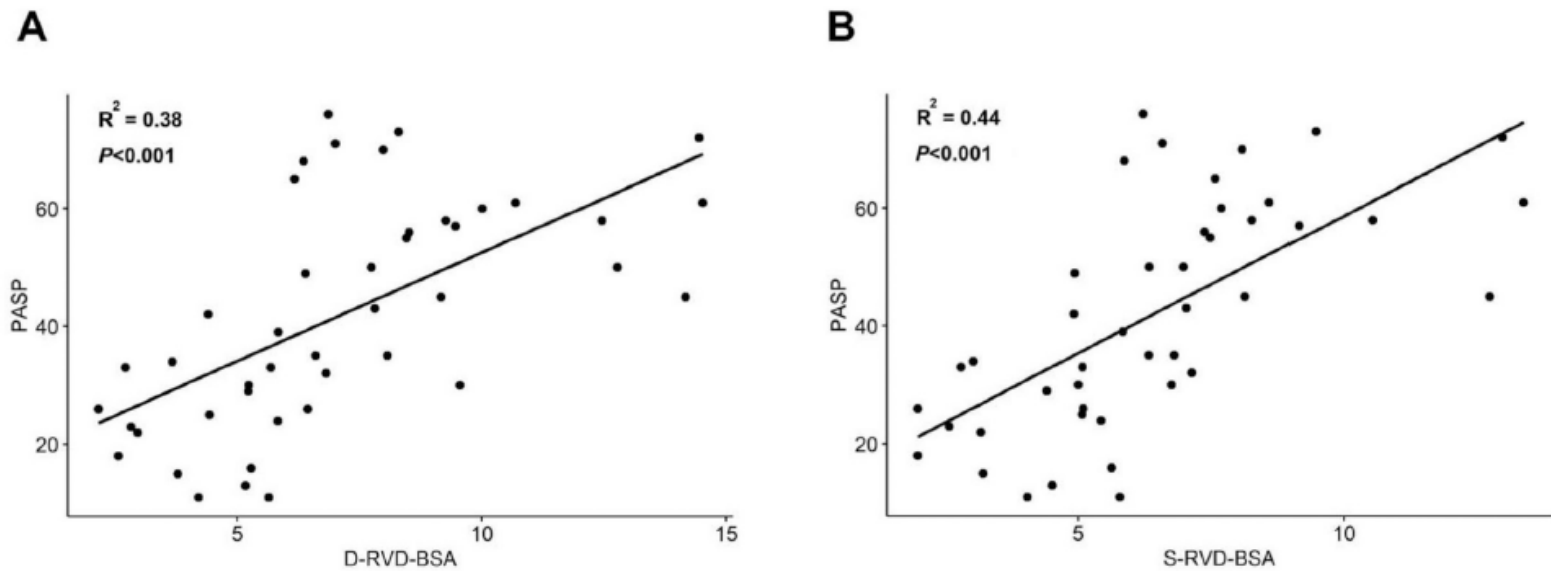# ECG-CTA-gated image parameters and associations with pulmonary pressures

Fig. 2. Correlations between D-RVD-BSA, S-RVD-BSA and PASP in all patients. Scatter plot showing relationship between D-RVD-BSA and PASP (A), and between S-RVD-BSA and PASP.

Table 2

Associations between measured parameters and PH.

Variable	Univariate OR (95% CI)	Multivariate[a] aOR (95% CI)
D-RVD-BSA	2.55 (1.45–4.48)	2.76 (1.23–6.23)
D-LVD-BSA	1.79 (1.26–2.56)	1.44 (0.93–2.24)
D-RVCSA-BSA	1.10 (1.00–1.22)	1.09 (0.95–1.24)
D-LVCSA-BSA	1.04 (0.96–1.12)	1.04 (0.95–1.14)
D-RVD/LVD	4.38 (0.54–35.39)	2.12 (0.27–16.87)
D-RVCSA/LVCSA	2.03 (0.58–7.07)	1.51 (0.38–5.97)
D-SEI	0.04 (<0.001–4.66)	0.08 (<0.001–13.19)
D-MPA/Ao	39.20 (2.62–586.80)	12.34 (0.59–257.02)
S-RVD-BSA	3.92 (1.70–9.05)	6.15 (1.72–22.06)
S-LVD-BSA	1.93 (1.26–2.97)	1.37 (0.78–2.41)
S-RVCSA-BSA	0.77 (0.64–0.94)	1.03 (0.79–1.35)
S-LVCSA-BSA	0.83 (0.70–0.97)	1.20 (0.85–1.69)
S-RVD/LVD	6.24 (0.60–64.91)	6.60 (0.32–135.26)
S-RVCSA/LVCSA	1.56 (0.50–4.87)	1.41 (0.36–5.58)
S-SEI	0.002 (<0.001–0.48)	0.002 (<0.001–0.51)
S-MPA/Ao	136.62 (7.33–>999)	74.51 (2.06–>999)

PH: pulmonary hypertension, OR: odds ratio, CI: confidence interval, D: diastolic, S: systolic, BSA: body surface area, RVD: right ventricular diameter, LVD: left ventricular diameter, RVCSA: right ventricular cross-sectional area, LVCSA: left ventricular cross-sectional area, SEI: septal eccentricity index; MPA/Ao: main pulmonary artery/ascending aorta ratio.

Number in bold indicate statistically significant results, $p < 0.05$.

[a] Models were adjusted for age and PDA.

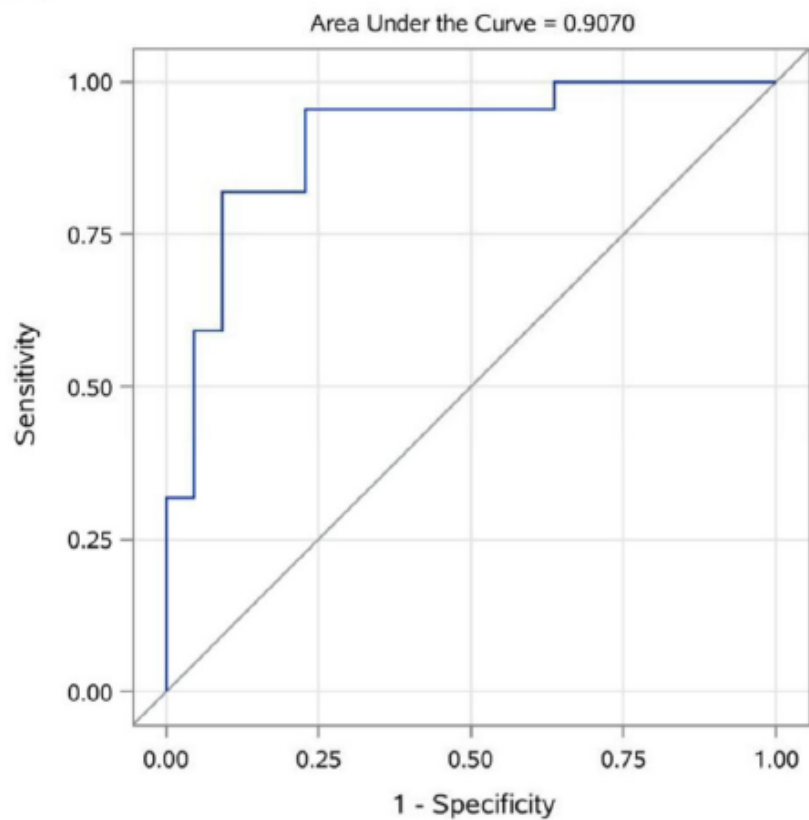Fig. 3. ROC curves for predicting pulmonary hypertension with D-RVD-BSA or S-RVD-BSA. The AUCs of the D-RVD-BSA (A) or S-RVD-BSA (B) for predicting pulmonary hypertension were 0.907 and 0.917, respectively.

- cut-off value of D-RVD-BSA and S-RVD-BSA for prediction of PH by ROC curve analysis was determined

- Area under the curve (AUC) of D-RVD-BSA was 0.907 and the AUC of S-RVDBSA was 0.917 (all p < 0.05)

Table 3
Associations between right ventricular diameter and PH.

Variable	Univariate	Multivariate[a]
	OR (95% CI)	aOR (95% CI)
D-RVD-BSA		
<6.86	1	1
≥6.86	**45 (7.34–275.76)**	**23.52 (2.89–191.03)**
S-RVD-BSA		
<5.87	1	1
≥5.87	**45 (7.34–275.76)**	**31.14 (2.75–352.85)**
D-MPA/Ao		
<1.18	1	1
≥1.18	**16.89 (3.63–78.53)**	**11.45 (1.85–70.79)**
S-MPA/Ao		
<1.32	1	1
≥1.32	**40.11 (7.17–224.45)**	NA

PH: pulmonary hypertension, OR: odds ratio, CI: confidence interval, D: diastolic, S: systolic, BSA: body surface area, RVD: right ventricular diameter; MPA/Ao: main pulmonary artery/ascending aorta ratio.

NA, Odds ratio could not be computed due to large odds ratio, aOR (95% CI) = >999 (<0.001->999).

Number in bold indicate statistically significant results, $p < 0.05$.

[a] Models were adjusted for age and PDA.

Radiation dose estimations

- The median CT dose index was 1.10 ± 0.84 mGy during prospective ECG-gated acquisition of each scan

- The average DLP provided by the CT system for estimating the radiation dose of one phase was 18.51 ± 21.67 mGy*cm. The average effective radiation dose of two phases in 44 patients was 2.82 ± 1.17 mSv (1.42 ± 0.57 mSv for one phase).

Discussion

- CHD is one of the leading etiologies of pediatric PH

- MDCT has been used increasingly for imaging patients with CHD because it provides high-quality three-dimensional images enabling evaluation of the complex heart structure and delivers a reasonable radiation dosage, especially in prospective ECG-gated CTA model (step-and-shoot mode)

- data on CT-based parameters for predicting PH in patients with CHD are scant, and only certain echocardiographic values are currently available

- In echocardiographic assessment of the right heart in adults, an RV basal dimension with an upper reference limit of 4.2 cm was determined to indicate RV dilation

- cut-off value of diastolic or systolic BSA-modified D-RVD (6.86) or SRVD (5.87) calculated by prospective ECG-gated CTA imaging is able to accurately predict PH in children with CHD

- CT has an important role in the diagnosis and follow-up of CHD, although it is used less frequently than echocardiography and cardiac magnetic resonance imaging (CMR) because of radiation and contrast exposure

- CT is the choice of imaging for patients with limited echocardiographic windows, claustrophobia when undergoing CMR, poor compliance, implantation of a pacemaker or implantable cardioverter defibrillator, or large metallic prostheses causing extensive artifacts on CMR

- present study confirms the potential of using parameters measured on prospective ECG-gated cardiac CTA for predicting pediatric PH with respect to the reference standard of the echocardiography-derived PASP

- Compared to retrospective ECG-gated computed tomography (CT), non-ECG-gated scanning technique is usually applied in CTA studies with low radiation dose in pediatric patients with CHD

A

Area Under the Curve = 0.8347

B

Area Under the Curve = 0.8864
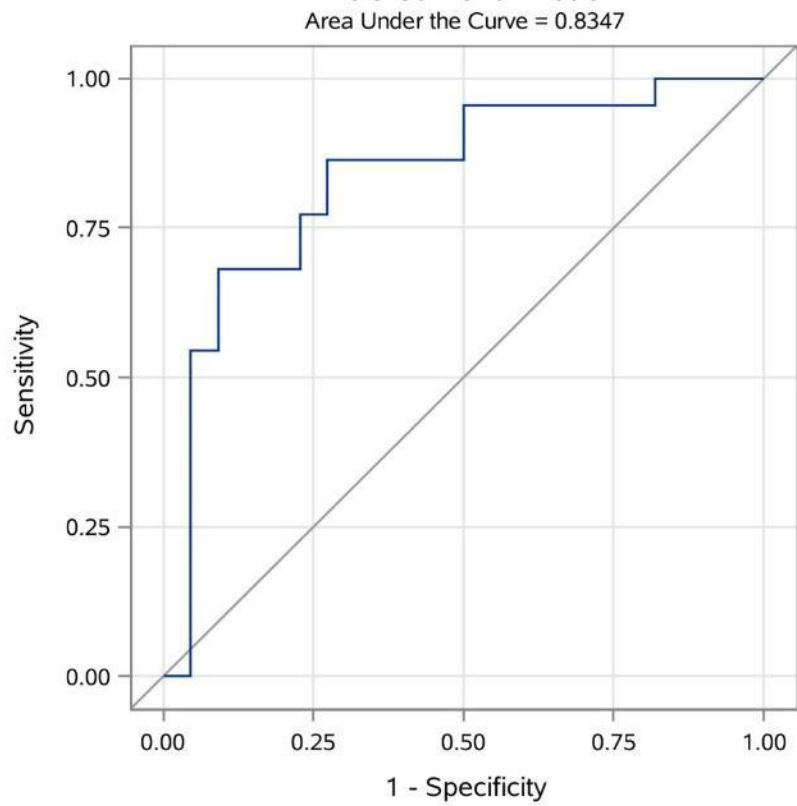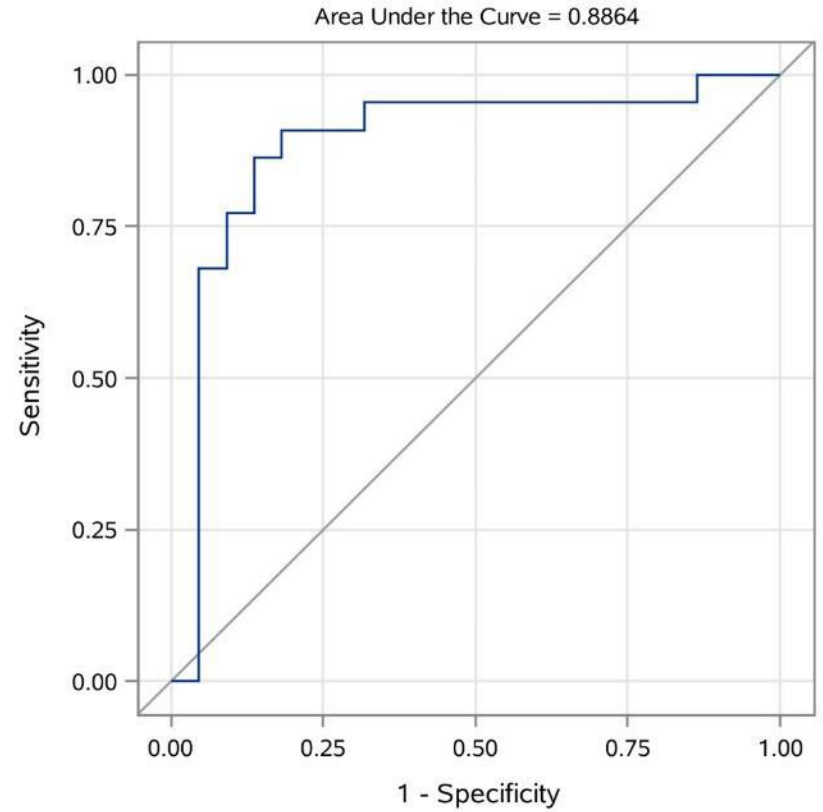
Limitation

- excluded CHD patients with pulmonary stenosis or RVOT obstruction. Therefore, the findings of this study cannot be extrapolated to a general CHD population.

- ECG-gated CTA protocols may have suboptimal quality related to various factors: different contrast enhancement in adjacent slice slabs, step artifacts due to movement in noncompliant patients, and respiratory artifacts in patients with poor breath holding

- the data acquisition windows in our cases are 70% and 30% of the R-R interval for diastole and systole, respectively, which did not represent the real situation in end-systole and end-diastole

- Although CT scans are not used in the longitudinal assessment of PH in children because of radiation exposure, functional CT parameters can provide quantitative information to supplement anatomic evaluations

Conclusion

- children with CHD, measurements of diastolic and systolic BSA-modified RVDs using prospective ECG-gated CTA are non-invasive markers of PH. BSA-modified D-RVD of 6.86 or BSA-modified S-RVD of 5.87 may be used to distinguish PH over 40 mm Hg in children with CHD

THANK YOU

JOURNAL CLUB

Presenter : Dr Rizwan Khan

Lecture in charge : Dr Khairil Amir Sayuti

Date : 04 January 2021
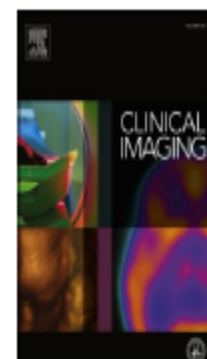
Cardiothoracic Imaging

Diastolic and systolic right ventricular diameters for predicting pulmonary hypertension in children with congenital heart disease

Bow Wang [a], Li-Ting Huang [a], Min-Ling Hsieh [b], Chien-Kuo Wang [a], Jieh-neng Wang [b], Chung-Dann Kan [c], Jing-Ming Wu [b], Yi-Shan Tsai [a,*]

[a] Departments of Diagnostic Radiology, National Cheng Kung University Hospital, College of Medicine, National Cheng Kung University, Tainan, Taiwan
[b] Departments of Pediatrics, National Cheng Kung University Hospital, College of Medicine, National Cheng Kung University, Tainan, Taiwan
[c] Department of Surgery and Institute of Cardiovascular Research Center, National Cheng Kung University Hospital, College of Medicine, National Cheng Kung University, Tainan, Taiwan

TITLE

Diastolic and systolic right ventricular diameters for predicting pulmonary hypertension in children with congenital heart disease

✔ Title gives good idea about study, measuring parameters used and target population

a Departments of Diagnostic Radiology, National Cheng Kung University Hospital, College of Medicine, National Cheng Kung University, Tainan, Taiwan

b Departments of Pediatrics, National Cheng Kung University Hospital, College of Medicine, National Cheng Kung University, Tainan, Taiwan

c Department of Surgery and Institute of Cardiovascular Research Center, National Cheng Kung University Hospital, College of Medicine, National Cheng Kung University, Tainan, Taiwan

✔ Different relevant departments and research center were involved

INTRODUCTION

Echocardiography is traditionally the first-line imaging modality used for patients with congenital heart disease (CHD)

✔ Expalined that truthfully

Right ventricular (RV) function determines both the degree of symptoms and survival among patients with PH, and RV failure remains the common fatal pathway and consequence of PH .

✔ Good justification for performing this study

Although defining PH is currently based on invasive cardiac catheterization, transthoracic echocardiogram is the initial diagnostic tool used to confirm suspicions of elevated pulmonary pressure when PASP is above 40 mm Hg

✔ Explained about gold standard investigation in clinical practice

✔ Expalined criteria for diagnosis on echocardiogram

PASP = pulmonary artery systolic pressure

Noninvasive Doppler echocardiography offers several variables that correlate closely with right heart hemodynamics, including PASP, therefore echocardiography PASP was applied as screening cutoff for defining suspected PH in this study.

Multidetector CT (MDCT) has been used increasingly for imaging patients with CHD, because it provides high-quality three-dimensional images enabling evaluation of complex heart structures.

 Also for critical cases with unstable hemodynamic status requiring examination with less life-threatening risk

✔ Explained gold standard technique (echocardiography) and criteria used in this study

✔ Explained usefulness of CT in target population

Previous studies have reported that several parameters obtained with cardiac CT, including the ratio of the main pulmonary artery (MPA) and the ascending aorta diameters (AA), the right ventricular maximal diameter, the ratio of right and left ventricular diameters, the ratio of right and left ventricular volumes, and the septal eccentricity index (SEI), can be used to predict PH in adults . To date, only few studies have presented useful parameters for predicting PH in children. For example, a CT measured MPA/AA of 1.3 was identified to be indicative of PAH in children by using non-gating 64-slice MDCT

However, functional parameters acquired using prospective ECG-gated cardiac CT to predict PH in children with CHD have not yet been reported.

✔ Explained that only few CT parameters are established for predicting PH in chidren

✔ Clearly explained limitations of CT

STUDY DESIGN AND POPULATION

The protocol for this retrospective study was approved by the institutional review board (IRB) of our hospital (B-ER-106-196), and the requirement for signed informed consent was waived due to the retrospective analysis and de identification of patients.

Prospective storage of raw prospective ECG-gated CTA data at our institution enabled retrospective reconstruction of the required image sets in this study.

✔ Got approval from IRB

✔ Study design clearly explained

PATIENTS

The cohort comprised 44 children with CHD with indications for CT and who received prospective ECG-gated cardiac CTA from September 2009 to September 2015

The exclusion criteria were: (a) CHD with right chambers involvement; (b) an unstable disease condition or no echocardiogram available within a 3-month period; (c) structural heart disease with right ventricular outlet tract (RVOT) obstruction; pulmonary valvular stenosis, or pulmonary artery stenosis, (d) unavailability of the PASP estimated through echocardiography, (e) unavailability of raw thin-slice CT data, and (f) suboptimal image quality.

No medication for heart rate control was used in this study group.

All included patients were divided into PH (n = 22) or non-PH (n = 22) groups on the basis of PASP > 40 mm Hg, as described previously

✔ Sample size, target population, inclusion sriteria and study duration explained

✔ Exclusion criteria clearly mentioned and valid

✘ Not reason given why no heart control medication used.

✔ Clearly explained how they divide patients

Fig. 1. Flow chart of the study population.
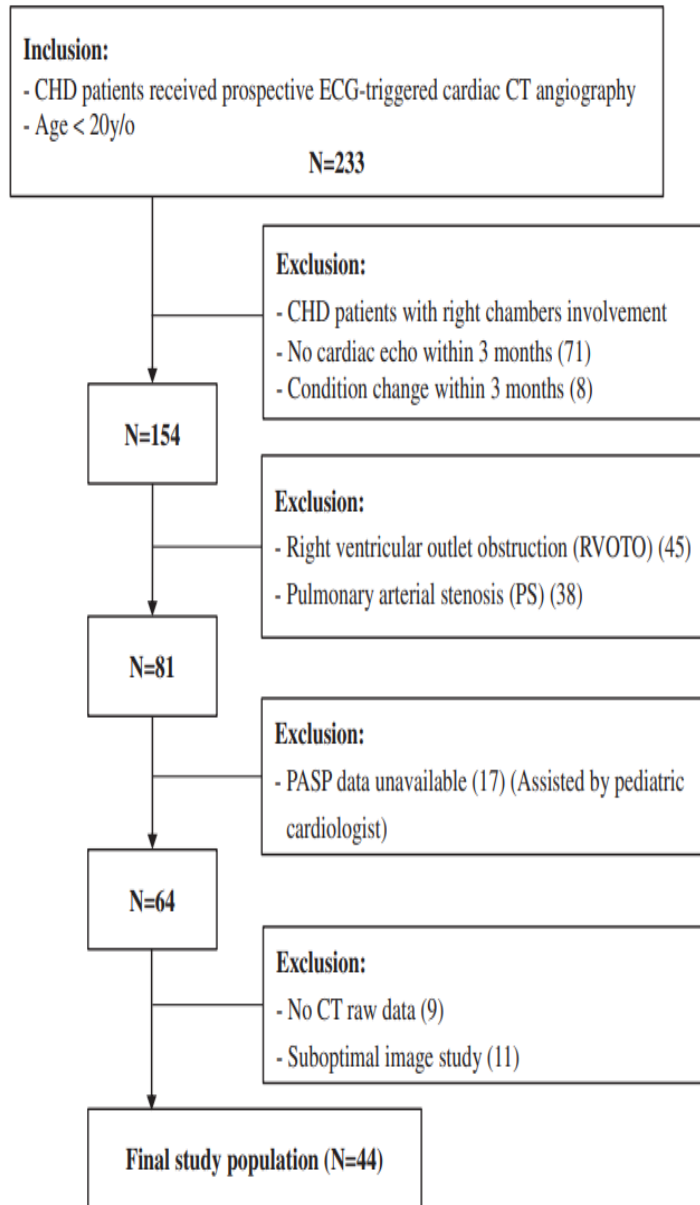
✔ Good explanation of inclusion and exclusion criteria with flow chart

CARDIAC CT PROTOCOL

Cardiac CT was performed with a dual-source CT system (Somatom Definition Flash; Siemens Healthcare, Forchheim, Germany) using the prospective ECG-gated scan mode (step-and-shoot scan mode). The CT parameters were as follows: detector collimation, 2 × 64 × 0.6 mm; slice acquisition, 2 × 128 × 0.6 mm using a z-flying focal spot; gantry rotation time, 280 ms; quality reference mAs, 150 per rotation; and tube voltage, 80 kV. A minimum cycle time of 1.36 s for one acquisition and a subsequent table feed were required, and the temporal resolution was 75 ms. Prior to the scan, patients who were unable to obey commands were sedated through oral or anal administration of chloral hydrate (50–75 mg/kg) according to the patient's body weight and clinical condition. All patients were scanned in a craniocaudal direction from the shoulder to the liver dome, to ensure inclusion of the subclavian artery and entire lung parenchyma. The nonionic contrast medium iopromide (Ultravist® 30, 370 mg/ml, Bayer Schering Pharma, Berlin, Germany) was injected through a peripheral venous line using a power injection. The volume injected was adjusted according to patients' body weight: 2–3 ml/kg contrast medium (CM), followed by a normal saline flush with one third of the amount of CM, with both being administered at a flow rate of 0.3–2.0 ml/s according to the size of intravenous access. For optimum vascular opacification, a round region of interest (ROI) was defined in the descending aorta. The triggered threshold of the ROI was set at 100 HU, and the image scan began after a delay of 7–9 s. The data acquisition window center was set at 70% and 30% of the R-R interval for diastole and systole, respectively.

✔ Procol is clearly mentioned. Protocol is valid and reproducible.

IMAGE ANALYSIS

One-millimeter thin-slice CTA images were analyzed using semiautomated postprocessing three-dimensional viewer software (Aquarius iNtuition Edition Ver: 4.4.7; TeraRecon, San Mateo, CA). For this study, the selected parameters were analyzed by two independent readers, B. W. and Y.S.T., with 3 and 14 years of experience in cardiothoracic imaging, respectively, and who were unaware of the PASP or the underlying disease. All images were initially analyzed by an experienced cardiac radiologist, including disease classification. Measurements of parameters for the images were performed by a pediatric radiologist. To determine the intra-observer variability, the same pediatric radiologist analyzed the images for all patients 1 month later. All data used to analyze data from the first and second analyses were averaged to minimize intra-observer variability. In addition, an experienced cardiac radiologist, who was blinded to the initial analysis, re-evaluated the images of 50% of the patients, who were chosen at random, to determine interobserver variability.

✔ Slice thickness chosen and software used explained.

✔ Experienced cardiac radiologist and pediatric radiologist involved.

✔ Clearly explained how intra observer and interobserver variability determined

On two sets of images (by default, the 30% and 70% of the R-R interval), a user-selected short-axis two-chamber view was reformed to be perpendicular to the long axis of the left ventricle (LV). The plane was moved until the papillary muscle was no longer visible, and a user selected apical four-chamber view was then reformed to visualize the maximal ventricular diameter and cross-sectional area (CSA)

The modified diameter and CSA were calculated as the RVD and LVD divided by the body surface area (BSA) and the RVCSA and LVCSA divided by the BSA, respectively; measurements were obtained in both systole and diastole.

✔ Good explanation using diagram and reproducible

SEI (systolic eccentricity index): higher SEI reflects higher PA pressure, with reported thresholds for PH (>1.3).

SEI was calculated as the ratio of the distance between the septal–lateral wall and the anterior–posterior wall measured in the short-axis view. Diameter measurements were obtained from the short-axis two-chamber view, which was adjusted at the mitral chordal insertion level.
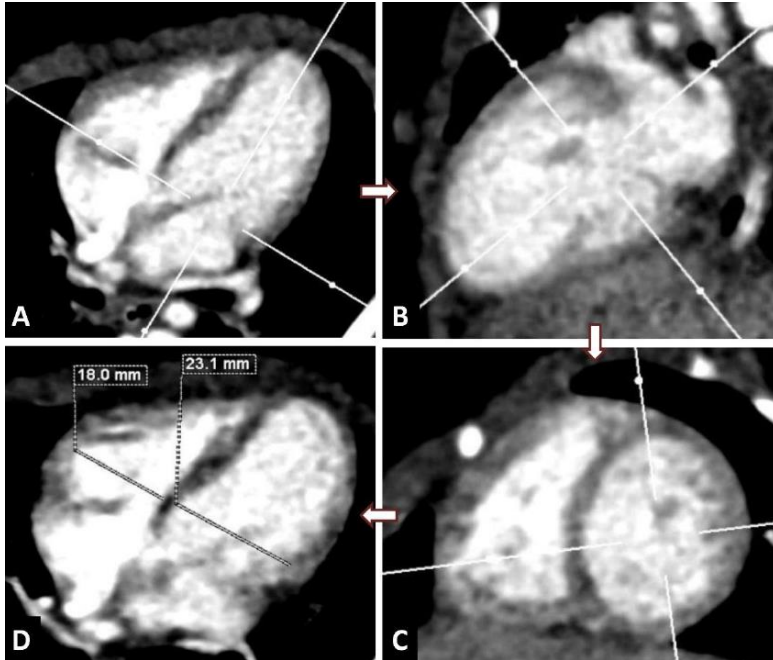
Fig. 1. Measurement of ventricular diameter through ECG-gated cardiac CTA. Based on user-selected reference points for the location of the valvular annulus, the software renders a three-dimensional estimate of the ventricular cavity (A → B). The observer then visually reviews and vertically cuts the left ventricular wall and reconstructs the two-chamber view (B → C). The cutting plane is moved until the papillary muscle is no longer visible and the four-chamber view is reconstructed. RV and LV dimensions are measured by identifying the maximal distance between the ventricular endocardium and the interventricular septum, perpendicular to the long axis (C → D).

Fig. 2. Measurements of ventricular CSA through ECG-gated cardiac CTA. Once the ventricles are properly segmented in the four-chamber view, the software manually calculates the ventricular CSA for both the RV and LV

Fig. 3. Measurement of eccentricity index through ECG-triggered cardiac CTA. Based on user-selected reference points for the location of the valvular annulus, the software renders a three-dimensional estimate of the ventricular cavity (A → B). The observer then visually reviews and vertically cuts the left ventricular wall and reconstructs the two-chamber view (B → C). The cutting plane is adjusted at the mitral chordal level, and the SEI is obtained as a ratio of the distance between the septal–lateral wall and the anterior–posterior wall measured in the short-axis view (C → D).
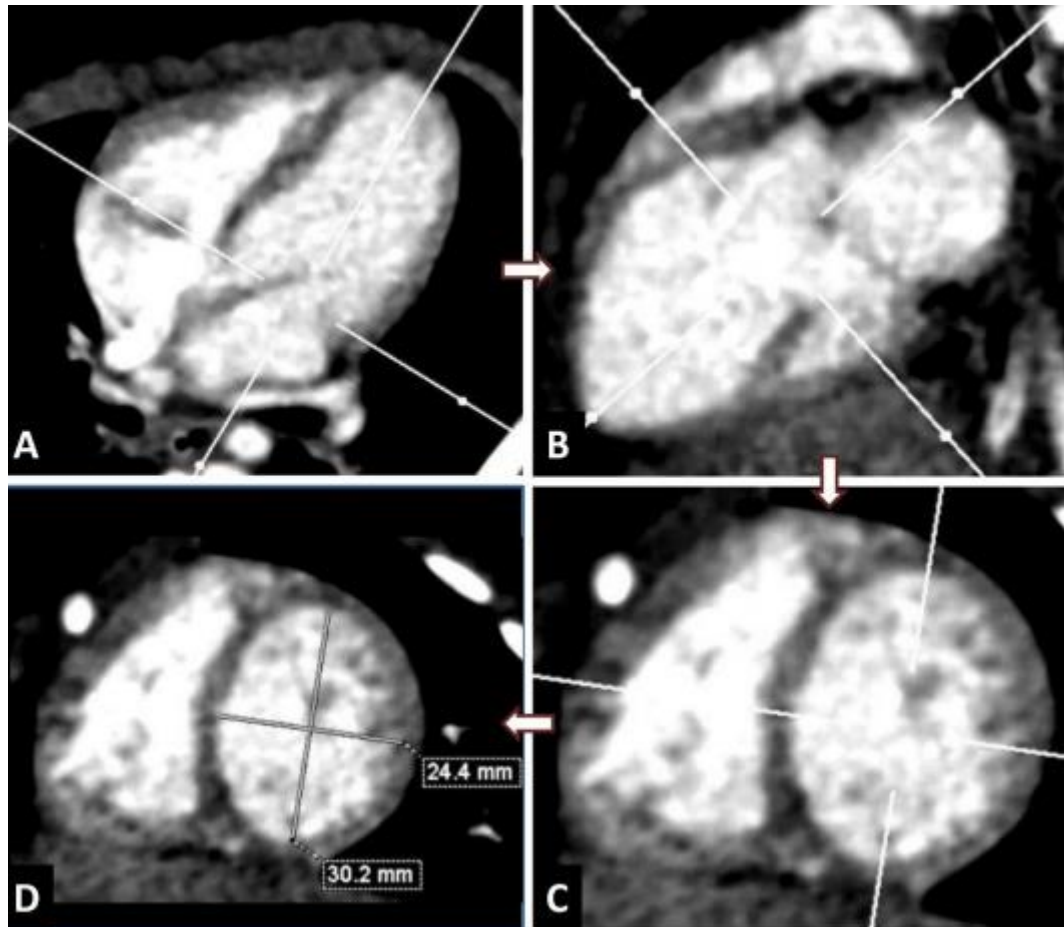
Interobserver agreement and interrater reliability

Good to excellent agreement between the results of the two observers was attained regarding functional parameters in the cardiac CT scans of 44 patients (Cohen's Kappa 0.625–0.821).

In addition, the consistency of one observer's measurements of functional parameters was good (Pearson correlation coefficient: 0.772–0.980).

✔ Good inter observer agreement and intra observer consistency was noted in measurment seems easy and reproducible measurement of parameters

Radiation dose

To assess the radiation dose, the effective dose in millisieverts was estimated by multiplying the dose-length product (DLP) by 2.3, because the machine uses a 32-cm phantom to evaluate the BSA. The effective radiation dose delivered during a chest CTA was calculated using International Commission on Radiological Protection publication 103 to determine the CT conversion factor. Conversion factors were 0.0823 for newborns, 0.0525 for 1-year old infants, 0.0344 for children aged 1–5 years, 0.0248 for children aged 5–10 years, and 0.0147 for children older than 10 years, and were based on a scan tube voltage of 80.

✔ Radiation dose calculation method clearly mentioned.

✔ Standard reference

Statistical analysis

Continuous variables are presented as mean and standard deviations (SDs) for normal distribution and tested by t-test or median and interquartile range (IQR) for non-normal distribution and tested by KruskalWallis test; categorical variables are presented as counts and percentages and tested by Chi-square test or Fisher's Exact test. The associations between measured parameters and PH were evaluated by logistic regression and baseline characteristics that were significantly different between the PH group and non-PH group were selected into multivariate logistic regression for adjustment. In addition, the receiver operating characteristic (ROC) curve was used to find the best cut-off point for parameters measured by Youden's index. Interrater reliability (IRR) was assessed using Kappa statistics. IRR was poor, fair, good, and excellent for Cohen's Kappa values from 0.0 to 0.2 indicating slight agreement, 0.21 to 0.40 indicating fair agreement, 0.41 to 0.60 indicating moderate agreement, 0.61 to 0.80 indicating substantial agreement, and 0.81 to 1.0 indicating almost perfect or perfect agreement, as previously described . The intrarater reliability was evaluated on the basis of test–retest reliability, and a Pearson correlation coefficient of >0.7 indicated good consistency . All statistical analyses were two-tailed and were performed using SAS version 9.4 (SAS Institute, Inc., Cary, NC, B. Wang et al. Clinical Imaging 70 (2021) 67–73 70 USA). A p value of <0.005 was established as a statistical significance.

✔ Statistical tests clearly mentioned

✔ Appropriate statistical methods used

✔ Statistical methods seems reproducible

✔ Software used clearly mentioned

Results

Table 1
Characteristics of the study population.

Variable	Non-PH group N = 22	PH group N = 22	p-Value
Age, months	36 (8, 84)	1 (0.13, 5)	<0.0001[a,*]
Sex			
Female	11 (50%)	10 (45.45%)	0.76[b]
Male	11 (50%)	12 (54.55%)	
Diagnosis			
ASD	7 (31.82%)	13 (59.09%)	0.07[b]
VSD	10 (45.45%)	16 (72.73%)	0.07[b]
CoA	3 (13.64%)	4 (18.18%)	1.00[c]
PDA	2 (9.09%)	10 (45.45%)	0.01[b,*]
TAPVR/PAPVR	2 (9.09%)	3 (13.64%)	1.00[c]
PASP	25.45 ± 8.44	58.41 ± 10.39	<0.0001[d,*]
D-RVD-BSA	5.02 ± 1.86	9.22 ± 2.87	<0.0001[d,*]
D-LVD-BSA	5.57 ± 2.38	8.77 ± 2.38	<0.0001[d,*]
D-RVCSA-BSA	18.79 ± 6.52	23.45 ± 7.87	0.04[d,*]
D-LVCSA-BSA	21.07 (18.84, 25.15)	22.39 (19.64, 31.34)	0.36[a]
D-RVD/LVD	0.88 (0.74, 1.08)	1.01 (0.85, 1.13)	0.26[a]
D-RVCSA/LVCSA	0.71 (0.55, 1.21)	0.83 (0.66, 0.98)	0.28[a]
D-SEI	0.81 ± 0.11	0.75 ± 0.16	0.18[d]
D-MPA/Ao	1.13 (1.08, 1.24)	1.56 (1.26, 1.72)	0.0001[a,*]
S-RVD-BSA	4.62 ± 1.58	8.21 ± 2.39	<0.0001[d,*]
S-LVD-BSA	4.55 ± 2.14	6.87 ± 1.81	0.0004[d,*]
S-RVCSA-BSA	8.98 (5.68, 12.25)	3.99 (3.44, 5.08)	0.001[a,*]
S-LVCSA-BSA	8.45 (6.06, 13.85)	4.20 (2.48, 5.26)	0.0002[a,*]
S-RVD/LVD	0.96 (0.89, 1.19)	1.07 (0.99, 1.32)	0.05[a]
S-RVCSA/LVCSA	0.86 (0.74, 1.19)	0.89 (0.81, 1.29)	0.31[a]
S-SEI	0.90 ± 0.09	0.79 ± 0.19	0.02[d,*]
S-MPA/Ao	1.19 (1.10, 1.26)	1.66 (1.46, 1.84)	<0.0001[a,*]

Continuous variables are shown as median and interquartile range for non-normal distribution or mean and standard deviation (SD) for normal distribution; categorical variables are shown as count and percentage.
PH: pulmonary hypertension, ASD: atrial septal defect, VSD: ventricular septal defect, CoA: coarctation, PDA: patent ductus arteriosus, TAPVR/PAPVR: total/partial anomalous pulmonary venous return, PASP: pulmonary arterial systolic pressure, D: diastolic, S: systolic, BSA: body surface area, RVD: right ventricular diameter, LVD: left ventricular diameter, RVCSA: right ventricular cross-sectional area, LVCSA: left ventricular cross-sectional area, SEI: septal eccentricity index; MPA/Ao: main pulmonary artery/ascending aorta ratio.
[a] Kruskal-Wallis test.
[b] Chi-square test.
[c] Fisher's Exact test.
[d] t-Test.
[*] p < 0.05.

✖ Did not explain why S-RVCSA and S-LVCSA-BSA values were low in PH patients

Table 2

Associations between measured parameters and PH.

Variable	Univariate	Multivariate[a]
	OR (95% CI)	aOR (95% CI)
D-RVD-BSA	2.55 (1.45–4.48)	2.76 (1.23–6.23)
D-LVD-BSA	1.79 (1.26–2.56)	1.44 (0.93–2.24)
D-RVCSA-BSA	1.10 (1.00–1.22)	1.09 (0.95–1.24)
D-LVCSA-BSA	1.04 (0.96–1.12)	1.04 (0.95–1.14)
D-RVD/LVD	4.38 (0.54–35.39)	2.12 (0.27–16.87)
D-RVCSA/LVCSA	2.03 (0.58–7.07)	1.51 (0.38–5.97)
D-SEI	0.04 (<0.001–4.66)	0.08 (<0.001–13.19)
D-MPA/Ao	39.20 (2.62–586.80)	12.34 (0.59–257.02)
S-RVD-BSA	3.92 (1.70–9.05)	6.15 (1.72–22.06)
S-LVD-BSA	1.93 (1.26–2.97)	1.37 (0.78–2.41)
S-RVCSA-BSA	0.77 (0.64–0.94)	1.03 (0.79–1.35)
S-LVCSA-BSA	0.83 (0.70–0.97)	1.20 (0.85–1.69)
S-RVD/LVD	6.24 (0.60–64.91)	6.60 (0.32–135.26)
S-RVCSA/LVCSA	1.56 (0.50–4.87)	1.41 (0.36–5.58)
S-SEI	0.002 (<0.001–0.48)	0.002 (<0.001–0.51)
S-MPA/Ao	136.62 (7.33–>999)	74.51 (2.06–>999)

PH: pulmonary hypertension, OR: odds ratio, CI: confidence interval, D: diastolic, S: systolic, BSA: body surface area, RVD: right ventricular diameter, LVD: left ventricular diameter, RVCSA: right ventricular cross-sectional area, LVCSA: left ventricular cross-sectional area, SEI: septal eccentricity index; MPA/Ao: main pulmonary artery/ascending aorta ratio.

Number in bold indicate statistically significant results, $p < 0.05$.

[a] Models were adjusted for age and PDA.

Results of univariate analysis showed that patients with higher RVD-BSA (systolic and diastolic) and LVD-BSA (systolic and diastolic) had higher risk of PH

Patients with higher S-RVCSA-BSA, S-LVCSA-BSA, or SSEI had lower risk of PH

However, results of multivariate analysis only remained significant in RVD-BSA (diastolic and systolic) after adjusting for age and PDA

✖ Did not explained reason for above findings.

Table 3

Associations between right ventricular diameter and PH.

Variable	Univariate	Multivariate[a]
	OR (95% CI)	aOR (95% CI)
D-RVD-BSA		
<6.86	1	1
≥6.86	**45 (7.34–275.76)**	**23.52 (2.89–191.03)**
S-RVD-BSA		
<5.87	1	1
≥5.87	**45 (7.34–275.76)**	**31.14 (2.75–352.85)**
D-MPA/Ao		
<1.18	1	1
≥1.18	**16.89 (3.63–78.53)**	**11.45 (1.85–70.79)**
S-MPA/Ao		
<1.32	1	1
≥1.32	**40.11 (7.17–224.45)**	NA

PH: pulmonary hypertension, OR: odds ratio, CI: confidence interval, D: diastolic, S: systolic, BSA: body surface area, RVD: right ventricular diameter; MPA/Ao: main pulmonary artery/ascending aorta ratio.

NA, Odds ratio could not be computed due to large odds ratio, aOR (95% CI) = >999 (<0.001->999).

Number in bold indicate statistically significant results, $p < 0.05$.

[a] Models were adjusted for age and PDA.

Logistic regression showed that patients with D-RVD-BSA over 6.86 had significantly higher risk of PH and the result remained significant after adjustment. Patients with S-RVD-BSA over 5.87 had significantly higher risk of PH and the result remained significant after adjustment

✔ Clearly explained

Radiation dose

The median CT dose index was 1.10 ± 0.84 mGy during prospective ECG-gated acquisition of each scan.

The average DLP provided by the CT system for estimating the radiation dose of one phase was 18.51 ± 21.67 mGy*cm.

The average effective radiation dose of two phases in 44 patients was 2.82 ± 1.17 mSv (1.42 ± 0.57 mSv for one phase).

✔ Clearly explained radiation dose

- However, this appears to be higher than previously reported sub-millisievert radiation doses, which we attribute to our use of rigorous conversion and correction factors in CT radiation estimation. However, the mean CT dose index and DLP were 1.10 mGy and 18.51 mGy*cm, respectively; these values are quite similar to radiation data from other prospective ECG-gated acquisitions

✔ Clearly explained likely cause of discrepancy in radiation dose

Supplementary Table 1. Heart rate of the study population by age group

	No. of patient	Heart Rate (mean±SD)
Total	44	117.48±25.03
Age Group		
Neonate	11 (27.5)	148.27±16.28
Infant	17 (38.6)	120.94 ±10.44
Children	13 (29.6)	96.15 ± 9.30
Adolescent	3 (6.8)	77.33 ± 9.88

Age group definition: Neonate, from birth to 1month; Infant, 1month to 2years; Children, 2 to 12years; Adolescent, 12 to 18years.

Heart rates are shown as mean and standard deviation (SD); Patient number are shown as count and percentage.

✔ Clearly explained heart rate in different age groups

Discussion

Recently, MDCT has been used increasingly for imaging patients with CHD because it provides high-quality three-dimensional images enabling evaluation of the complex heart structure and delivers a reasonable radiation dosage, especially in prospective ECG-gated CTA model (step-and-shoot mode)

✔ Good explanation for doing MDCT in pediatrics patients with CHD

Data on CT-based parameters for predicting PH in patients with CHD are scant, and only certain echocardiographic values are currently available .

In the present study, pediatric patients with CHD who had increased D-RVD-BSA or S-RVD-BSA had higher risk of PH. In particular, the cutoff values of 6.86 and 5.87 for the diastolic and systolic BSA-modified RVDs had higher sensitivities and specificities to predict the occurrence of PH in these patients. This suggests that D-RVD-BSA and S-RVD-BSA may be useful biomarkers for predicting PH in children with CHD.

✔ Good explanation of usefulness of study

CT is the choice of imaging for patients with (1)limited echocardiographic windows,

(2) claustrophobia when undergoing CMR,

(3) poor compliance,

(4) implantation of a pacemaker or implantable cardioverter defibrillator, or large metallic prostheses causing extensive artifacts on CMR.

✔ Good conditions provided for using CT in place of echocardiography and MRI

Limitations

(1) First, we excluded CHD patients with pulmonary stenosis or RVOT obstruction. Therefore, the findings of this study cannot be extrapolated to a general CHD population.

(2) Second, ECG-gated CTA protocols may have suboptimal quality related to various factors: different contrast enhancement in adjacent slice slabs, step artifacts due to movement in noncompliant patients, and respiratory artifacts in patients with poor breath holding .

(3) Third, the data acquisition windows in our cases are 70% and 30% of the R-R interval for diastole and systole, respectively, which did not represent the real situation in end-systole and end-diastole

✔ Clearly explained limitations

Conclusion

In children with CHD, measurements of diastolic and systolic BSA modified RVDs using prospective ECG-gated CTA are non-invasive markers of PH. BSA-modified D-RVD of 6.86 or BSA-modified S-RVD of 5.87 may be used to distinguish PH over 40 mm Hg in children with CHD.

✔ Good conclusion of using low dose CT for predicting PH in particular situations where echocardiography and MRI can not be performed

Table 4 The seven rules for an optimised CT dose reduction in children. *CTDI* CT dose index, *DLP* dose-length product, *US* ultrasound, *MRI* magnetic resonance imaging, *HRCT* high-resolution computed tomography

1 Justify CT examination rigourously
- respect age-specific pathology and its prognosis
- respect individual paediatric questions
- consider potential contribution of the scan to the management and outcome
- respect cost and radiation exposure
- replace CT by examination without (US, MRI) or with lower radiation exposure
- delay follow-up examination unless therapeutic decision based on scan is needed now

2 Prepare the patient
- informed consent (parents)
- check renal function and verify hydration
- place intravenous line well in advance
- decrease anxiety; calm patient (information, accompanying person)
- mark bowel (for abdominal scan)
- avoid pain (immobilisation, positioning, medication)
- sedate, anaesthetise
- prepare monitoring, such as oximetry
- exercise cooperation without radiation
- put protective device where indicated (lens, thyroid, breast, gonads)

3 Accept noise as long as the scan is diagnostic
- realise that in digital X-ray imaging, noise reduction requires higher exposure
- reduce mAs (and possibly kV)
- reconstruct additional thick noise-reduced slices without increase of exposure

4 Optimise scan parameters within the axial plane
- increase tube filtration (if available)
- use maximal slice thickness appropriate for specific diagnosis
- decrease kVp for thin objects
- use shortest rotation time available (only few exceptions in children)
- decrease baseline mA (CTDI) according to body diameter and composition
- use XY-plane dose modulation to minimise CTDI

5 Optimise scan parameters for volume coverage
- use representative volume sample when entire volume is not needed (by sequential scans with gaps) to reduce DLP
- use spiral scan with pitch >1 (e.g. 1.5) to reduce DLP
- use thicker collimation with overlapping reconstruction when thin slices are not needed
- use Z-axis dose modulation to decrease DLP
- in the near future, use noise-defined automatic exposure control

6 Scan minimal length
- be restrictive in defining upper-most and lower-most limits to keep DLP low
- use localising projection scan extending just minimally beyond scan limits

7 Minimise repeated scanning of identical area
- avoid major overlap when scanning adjacent areas with different protocols
- avoid non-enhanced scans unless specifically justified (e.g. for densitometry)
- optimise the protocol to obtain all the information requested during one scan (e.g. contiguous 5 mm images and 1 mm HRCT images every 10 mm); minimise number of scans in multi-phase scanning to decrease DLP
- in case of multi-phase scanning, use shorter scan length for additional scans
- use lower CTDI for non-enhanced or repeat scans unless high quality is needed
- use minimal number of additional sequential functional scans to keep DLP low
- minimise length of scans and fluoroscopy time in interventional applications
- replace test bolus/bolus triggering by standard scan delay unless timing is very critical

Table 1 Summary of CTDIvol and effective dose values as reported by different authors as discussed in the review together with data from our Institution

From: [Paediatric cardiac computed tomography: a review of imaging techniques and radiation dose consideration](#)

	Age	Weight kg	Retrospective ECG-Triggered Study			Prospective ECG-Triggered Study			Non-Gated Study		
			CTDIvol mGy	DLP mGy*cm	EffectiveDose mSv	CTDIvol mGy	DLP mGy*cm	EffectiveDose mSv	CTDIvol mGy	DLP mGy*cm	EffectiveDose mSv
TSAI	1month	2.9		91.2 ± 11.4							
CHENG	2m–6y	2.5–15				1.39 ± 0.4 (0.83–1.92)	20 ± 6 (10–32)	0.38 ± 0.1 (0.25–0.58)			
JIN	1d–5y	2.5–16	3.41 ± 0.78	46.64 ± 16.1	0.79 ± 0.27	1.33 ± 0.13	12.5 ± 3.71	0.21 ± 0.06			
SAAD	1d–1y	2.4–9		21 ± 9 (10–39)	1.3 ± 0.6 (0.6–2.8)					8 ± 6 (4–18)	0.5 ± 2 (0.2–0.9)
PAUL	1d–5.4y	1.8–21					5.7 ± 4.8 (1–22)	0.26 ± 0.16 (0.05–0.8)			
GOSH	1d–4.5y	2–14.3	1.83 ± 0.8 (0.68–4.2)	28 ± 11 (10–52)	1.9 ± 0.7 (0.8–8)	0.92 ± 0.3 (0.32–1.33)	11 ± 3.3 (3–16)	0.7 ± 0.2 (0.3–1.3)	0.76 ± 0.1 (0.6–1.0)	12 ± 4 (6–22)	0.9 ± 0.2 (0.54–1.4)

Table 2:

Strengths and weaknesses of cardiac CT, cardiac MRI, echocardiography, and cardiac catheterization in children

Modality	Spatial Resolution	Temporal Resolution	Availability	Exam time	Invasiveness	Cost	Need for Contrast Media	Field-of-view limitation	Contra-indications	Porta-bility	Sedation	Ease of monitoring patients during exam
Cardiac CT	++	+	++	+	++	Intermediate	Yes	No	Yes	−	Occasionally	++
Cardiac MRI	+	++	+	++	++	Intermediate	Often	No	Yes	−	Typically below age 8	+
Echocardiography	++	+++	+++	++	+	Intermediate	Rarely	Yes	No	+++	Rarely	+++
Catheterization	+++	+++	++	+++	+++	High	Yes	No	Yes	−	Typically for all pediatric patients	+++

+ = low; ++ = moderate; +++ = high; − = not available

- Biological impact of low-level radiation Deterministic effects, i.e. those observed predictably above a certain threshold, are not seen below 100 mSv of local dose. Low-level radiation is mostly defined as ionising radiation in the range of up to 100 mSv of effective dose where only stochastic effects of ionising radiation are expected. Stochastic effects are those expected without any threshold and consisting mainly of radiation-induced cancers and genetic effects. Single CT examinations usually provide for less than 1 mSv to more than 27 mSv although in children, this upper threshold may well be exceeded, e.g. when adult protocols are used.

- The data show a statistically significant increase of the risk of fatal cancer starting at the range of 50– 100 mSv, possibly already at 10–50 mSv ; 100 mSv are expected to cause a lifetime risk of 0.5% for fatal cancer. A single, full-body CT scan (from C3 to the pubic symphysis) in a 45-year-old would cause an effective dose of about 12 mSv and an estimated lifetime cancer risk of 0.08% (95% confidence interval of 0.025–0.26%); should this be repeated for yearly screening, the same individual would run a 1.9% risk up to the age of 75 years

- Reasons for a greater risk in paediatric as compared with adult CT

  Higher biological sensitivity at same effective dose

  More proliferating tissues, different distribution

  Longer life expectancy Late manifestation of radiation-induced cancer

Reference

1. Wang, B., Huang, L.-T., Hsieh, M.-L., Wang, C.-K., Wang, J., Kan, C.-D., … Tsai, Y.-S. (2021). Diastolic and systolic right ventricular diameters for predicting pulmonary hypertension in children with congenital heart disease. Clinical Imaging, 70, 67–73.

2. Vock, P. (2005). *CT dose reduction in children. European Radiology, 15(11), 2330–2340.* doi:10.1007/s00330-005-2856-0.

3. Young, C., Taylor, A. M., & Owens, C. M. (2010). *Paediatric cardiac computed tomography: a review of imaging techniques and radiation dose consideration. European Radiology, 21(3), 518–529.* doi:10.1007/s00330-010-2036-8.

4. Rigsby, C. K., McKenney, S. E., Hill, K. D., Chelliah, A., Einstein, A. J., Han, B. K., … Frush, D. P. (2018). *Radiation dose management for pediatric cardiac computed tomography: a report from the Image Gently "Have-A-Heart" campaign. Pediatric Radiology, 48(1), 5–20.*

5. Vock, P. (2005). *CT dose reduction in children. European Radiology, 15(11), 2330–2340.* doi:10.1007/s00330-005-2856-0